The *Arf* tumor suppressor gene promotes hyaloid vascular regression during mouse eye development

Robyn N. McKeller*, Jennifer L. Fowler*, Justine J. Cunningham†, Nikita Warner*, Richard J. Smeyne†, Frederique Zindy‡, and Stephen X. Skapek*§

Departments of *Hematology/Oncology, †Developmental Neurobiology, and ‡Tumor Cell Biology, St. Jude Children's Research Hospital, 332 North Lauderdale Street, Memphis, TN 38105

A key tumor suppressor mechanism that is disrupted frequently in human cancer involves the *ARF* and *p53* genes. In mouse fibroblasts, the *Arf* gene product responds to abnormal mitogenic signals to activate p53 and trigger either cell cycle arrest or apoptosis. Recent evidence indicates that *Arf* also has *p53*-independent functions that may contribute to its tumor suppressor activity. Using *Arf*−/− and *p53*−/− mice, we have discovered a *p53*-independent requirement for *Arf* in the developmental regression of the hyaloid vascular system (HVS) in the mouse eye. *Arf* is expressed in the vitreous of the eye and is induced before HVS regression in the first postnatal week. In the absence of *Arf*, failed HVS regression causes a pathological process that resembles persistent hyperplastic primary vitreous, a developmental human eye disease thought to have a genetic basis. These findings demonstrate an essential and unexpected role for *Arf* during mouse eye development, provide insights into the potential genetic basis for persistent hyperplastic primary vitreous, and indicate that *Arf* regulates vascular regression in a *p53*-independent manner. The latter finding raises the possibility that *Arf* may function as a tumor suppressor at least in part by regulating tumor angiogenesis.

The capacity to induce new blood vessels by the process of angiogenesis is an essential feature of malignant tumors (1–3). During malignant tumorigenesis, this "angiogenic switch" may be driven by alterations in the balance of a number of pro- or antiangiogenic factors (2, 3). For example, angiogenesis can be triggered by an excess of proangiogenic peptide growth factors such as fibroblast growth factors 1 and 2, vascular endothelial growth factors (VEGFs), and angiopoietin-1 (Ang-1) or by a deficiency of antiangiogenic factors, such as thrombospondin-1 (3–6). In principle, any event that shifts this balance against angiogenesis might contribute to tumor suppression.

One of the most important tumor suppressor mechanisms involves the *Arf*, *Mdm2*, (*HDM2* in humans), and *p53* genes (7, 8). The p53 protein functions as the main effector in this genetic and biochemical pathway. Although it induces the expression of thrombospondin-1 (9) and decreases the expression of VEGF (10, 11), most data indicate that p53 functions as a tumor suppressor by inducing cell cycle arrest or apoptosis in response to abnormal cellular and genotoxic stresses, including DNA damage, hypoxia, and aberrant cell-proliferation signals (8, 12). The *Mdm2* gene product functions in part by physically interacting with p53 to block its transcription-activation function (13, 14) and enhance its degradation (15, 16). *Arf* encodes p19^Arf (p14^ARF in humans), which is thought to function as a tumor suppressor by physically interacting with Mdm2 to stabilize p53 (17–19). This tumor suppressor pathway may be inactivated by genetic or epigenetic events that inactivate *p53* or *Arf* or activate the expression or function of *Mdm2*. Its critical importance is evidenced by the observation that at least one of its components is disrupted in most human cancers (7, 8).

The *Arf-Mdm2-p53* network initially was depicted as a linear pathway (7), but recent evidence suggests that p19^Arf has func-tions that are distinct from p53. For example, the tumor spectrum differs in *Arf*−/− and *p53*−/− mice in that sarcomas are more common in the former whereas lymphomas are more prevalent in the latter (20–22). Furthermore, ectopically expressed *Arf* can arrest proliferation of mouse embryonic fibroblasts that lack both *p53* and *Mdm2* (23). Cellular or molecular mechanisms by which *Arf* may have *p53*-independent tumor suppressor effects have not been established.

By studying mice lacking *Arf* and *p53*, we have identified a *p53*-independent requirement for *Arf* to promote regression of the hyaloid vascular system (HVS) during mouse eye development. The expression of *Arf* in the vitreous before HVS regression is consistent with this requirement. In the absence of *Arf*, mice develop eye abnormalities that mimic persistent hyperplastic primary vitreous (PHPV), a human developmental eye disease associated with failed HVS regression (24, 25). The development of PHPV in *Arf*−/− mice is independent of *p53*. Together, these findings suggest that abnormalities of human *ARF* may contribute to PHPV, and they raise the possibility that one component of *Arf*-dependent tumor suppression may be its ability to promote vascular regression.

Methods

Mice and Genotyping. *Arf*−/− mice (26) and *Arf*−/−, *p53*−/− mice (23) in a mixed C57BL/6 × 129/SvJ background were provided by M. Roussel and C. Sherr (St. Jude Children's Research Hospital); *p53* knockout mice in a similar mixed genetic background (22), purchased from The Jackson Laboratory, were provided by G. Grosveld ((St. Jude Children's Research Hospital). All studies were approved by the St. Jude Children's Research Hospital Animal Care and Use Committee.

Arf genotype was determined by PCR analysis of genomic DNA obtained by tail biopsy by using primers specific for the wild-type and targeted alleles as follows: 5′-AGTACAG-CAGCGGGAGCATGG (wild type), 5′-TTGAGGAGGAC-CGTGAAGCCG (wild type and targeted), and 5′-ACCA-CACTGCTCGACATTGGG (targeted). *p53* genotype was determined as described (22).

Reverse Transcriptase (RT)-PCR Analysis of Gene Expression. Total RNA was extracted from intact or fractions of mouse eyes, which were removed from euthanized mice and frozen immediately in liquid nitrogen. Fractions of mouse eyes were obtained by

manual dissection, using an operating microscope after enucleation and before freezing. RNA was extracted by using the Trizol reagent (Life Technologies, Gaithersburg, MD) according to the manufacturer's recommendations. Equivalent amounts of RNA from each sample were converted to cDNA by using Superscript II RT (Life Technologies). PCR was performed by using 10-fold dilutions of cDNA, using primers for *Arf* (27); rhodopsin (28); αA- and βB2-crystallins (29); interphotoreceptor retinoid-binding protein, 5′-GAAGCCCTCCAGGACTATTACACA and 5′-TCATTAGGCCCAGTCTCAGGTCTT; and glyceraldehyde-3-phosphate dehydrogenase (GAPDH), 5′-AGC-CAAAAGGGTCATCATCT and 5′-GGGGCCATCCA-CAGTCTTCT. After PCR, equal amounts of reaction product were fractionated by electrophoresis in ethidium bromide-containing agarose gels, which were photographed. For *Arf*, Southern blot was performed by using *Arf* exon 1β-specific cDNA probe as described (27).

Histological Studies. Eyes were removed from euthanized mice and fixed in 4% paraformaldehyde in PBS for 24 h and then embedded in paraffin. Five- to 6-μm-thick sections from paraffin blocks were used for hematoxylin/eosin (H&E) stain or for immunohistochemical studies by using monoclonal anti-smooth muscle α-actin antibody (Dako) and biotinylated Fab anti-mouse antibody (Dako), or rabbit anti-von Willebrand factor (anti-factor VIII-related antigen) antiserum (Dako) or rabbit anti-Ki-67 proliferating cell nuclear antigen (NovoCastra, Newcastle, U.K.) and biotinylated goat anti-rabbit antibody (Vector Laboratories). Biotinylated antigen–antibody complexes were detected by using streptavidin conjugated to horseradish peroxidase, the chromogen 3,3′-diaminobenzidine tetrahydrochloride, and hematoxylin counterstain, all obtained from Dako. Control experiments for immunohistochemical studies included sections processed in parallel by using unrelated primary antibodies of the appropriate species.

Digital photomicrographs of stained sections were obtained by using an Olympus BX60 microscope equipped with a SPOT RT Slider camera (Diagnostic Instruments, Sterling Heights, MI). Composite images were constructed by using PHOTOSHOP 5.0 software (Adobe Systems, Mountain View, CA).

Quantitative studies of thickness of outer and inner nuclear layers were performed by measuring their widths in representative midline sections within 250 μm of the optic nerve or by counting the number of ganglion cell nuclei in a 250-μm span adjacent to the optic nerve. The mean and SEM was determined from at least five values from three or four mice that were either *Arf*$^{-/-}$ or had at least one normal *Arf* allele. No differences were noted between *Arf*$^{+/-}$ and wild-type littermates in any analyses.

Results

Failed Regression of the HVS in *Arf*$^{-/-}$ Mice. *Arf*$^{-/-}$ mice were not noted previously to have developmental abnormalities (20, 26). However, we observed that the eyes of most *Arf*$^{-/-}$ mice were noticeably smaller than eyes of wild-type or *Arf*$^{+/-}$ littermates (data not shown). Histological studies revealed the presence of a funnel-shaped retrolental mass of cells present in the vitreous of *Arf*$^{-/-}$ eyes on postnatal day 1 (P1) through P10 (Fig. 1 *b*, *d*, and *g* and data not shown). The presence of Ki-67-positive cells in the retrolental tissue suggested that some of the cells were undergoing DNA replication from P1 through P10 (Fig. 1 *g* and *h* and data not shown). In addition, some cells in this tissue were undergoing apoptosis, as evidenced by terminal deoxynucleotidyltransferase-mediated UTP end labeling staining from P1 through P5 (data not shown). Retrolental tissue was observed in all *Arf*$^{-/-}$ mice, but not in wild-type (Fig. 1 *a*, *c*, and *e*) or *Arf*$^{+/-}$ littermates (data not shown). In some nonalbino *Arf*$^{-/-}$ mice, pigmented cells, which were stained by using the antimelanocyte HMB45 antibody (data not shown), were observed in the
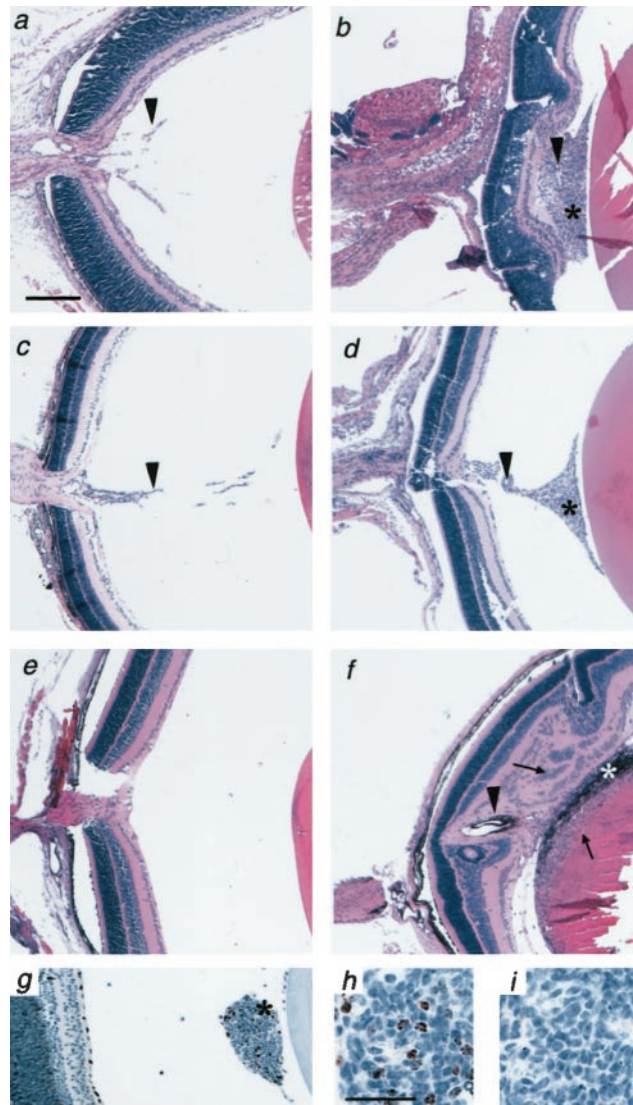

Fig. 1. Abnormal retrolental tissue present in the eyes of neonatal *Arf*$^{-/-}$ mice. Photomicrographs of sections of mouse eyes from wild-type (*a*, *c*, and *e*) and *Arf*$^{-/-}$ (*b*, *d*, and *f–i*) mice at P3 (*g–i*), P5 (*a* and *b*), P10 (*c* and *d*), and P14 (*e* and *f*). Sections were stained with H&E (*a–f*), anti-Ki-67 antibody (*g* and *h*), or unrelated primary antibody as a control (*i*). Note the presence of retrolental tissue (*), pigmented cells within the retrolental tissue in nonalbino mouse (*, *f*), hyaloid vessels (arrowhead) in the vitreous (*a* and *c*) and retrolental tissue (*b*, *d*, and *f*), and neuroretina and lens abnormalities (arrows, *f*). Anterior is to the right. [Magnifications: ×40 (*a–f*), ×100 (*g*), and ×400 (*h* and *i*); bar = 200 μm (*a*) and 30 μm (*h*).]

retrolental tissue at P10 (data not shown) and P14 (Fig. 1*f*). The retrolental tissue adhered to the lens and neuroretina by P14 (Fig. 1*f*) and persisted, without apparent increase in size, in 2- to 8-month-old mice (see Fig. 4*i*).

Normally, the retrolental vitreous in the newborn mouse eye contains elements of the HVS. The HVS is composed of endothelial cells and several types of perivascular cells (30, 31) forming the hyaloid artery (HA), the vasa hyaloidea propria (VHP) branching from the HA, the tunica vasculosa lentis surrounding the lens, and the pupillary membrane (Fig. 2*a*). Within the retrolental tissue in *Arf*$^{-/-}$ mice, large vascular structures extended from the optic nerve toward the posterior lens, along the course of the HA (Fig. 2 *b–d*). The HA-like vessels were surrounded by perivascular cells that expressed smooth muscle α-actin (Fig. 2 *c* and *d*), which normally is found
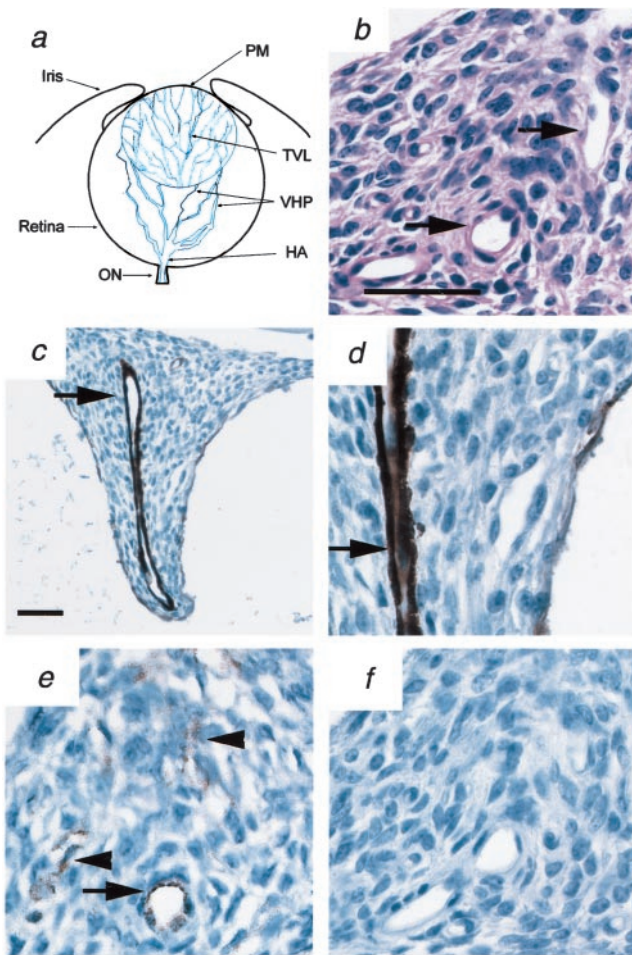
Fig. 2. Retrolental tissue in $Arf^{-/-}$ mice contains mature hyaloid vascular structures and endothelial cells. (*a*) Schematic diagram of hyaloid vessels in neonatal mouse eye. Adapted from ref. 31. (*b–f*) Representative photomicrographs of sections of retrolental mass in albino P10 $Arf^{-/-}$ mice. Sections were stained with H&E (*b*) or anti-smooth muscle α-actin for pericytes (*c* and *d*) or anti-von Willebrand factor (vWF) for endothelial cells (*e*) or unrelated primary (*f*) antibodies. Note the presence of large vascular structures within the retrolental tissue (arrows) and other scattered endothelial cells (arrowheads, *e*). [Magnifications: ×200 (*c*) and ×600 (*b* and *d–f*); bar = 50 μm (*b* and *c*).]

Fig. 3. Arf is expressed in the vitreous of the mouse eye during the early postnatal period. (*a*) Representative photograph of ethidium bromide-stained agarose gel [Arf (*Upper*) and GAPDH] and Southern blot [Arf (*Lower*)] of PCR products by using primers specific for Arf and GAPDH as indicated, showing the presence of Arf transcript from P1–P5. PCR was performed on 10-fold dilutions of cDNA (RT+) or undiluted RNA (RT−) made from total RNA extracted from whole eyes of P1, P3, P5, and P7 wild-type mice. (*b*) Representative photograph of Southern blot (top) and ethidium bromide-stained agarose gels (bottom three) of PCR products obtained by using primers specific for Arf, interphotoreceptor retinoid-binding protein (IRBP) (*Left*) or rhodopsin (*Right*), β-crystallin, and GAPDH as indicated. PCR was performed on cDNA (RT+) or RNA (RT−) from total RNA extracted from the lens (L), optic cup (OC), or vitreous (V) elements of the eye. *Left* and *Right* represent independent results from two separate mice.

in some mature pericytes (32, 33). The localization of mature pericytes around these vessels is consistent with previous studies of normal hyaloid vasculature (30). Some widely scattered cells in the retrolental tissue expressed endothelial markers von Willebrand factor (Fig. 2*e*) and CD34 (data not shown). Taken together, these findings indicated that the retrolental tissue was composed, in part, of mature hyaloid vessels and endothelial cells as either immature vessels or capillaries.

It is important to note that the mouse HVS normally regresses during the first 2 weeks of postnatal development (31). Indeed, in wild-type littermates, we did not observe a remnant HVS after P10 (Fig. 1 *a*, *c*, and *e*). Hence, the presence of the mature, HA-like vessels and endothelial cells in the retrolental tissue indicated that the HVS failed to regress in $Arf^{-/-}$ mice.

Arf Is Expressed in the Vitreous Before Hyaloid Vascular Regression. Most of the retrolental tissue was located within the region of the VHP (Figs. 1 and 2*a*), which normally regresses between P6 and P10 in the mouse (ref. 31 and data not shown). Therefore, we considered that Arf might specifically promote VHP regression. To begin to evaluate this notion, we characterized the temporal
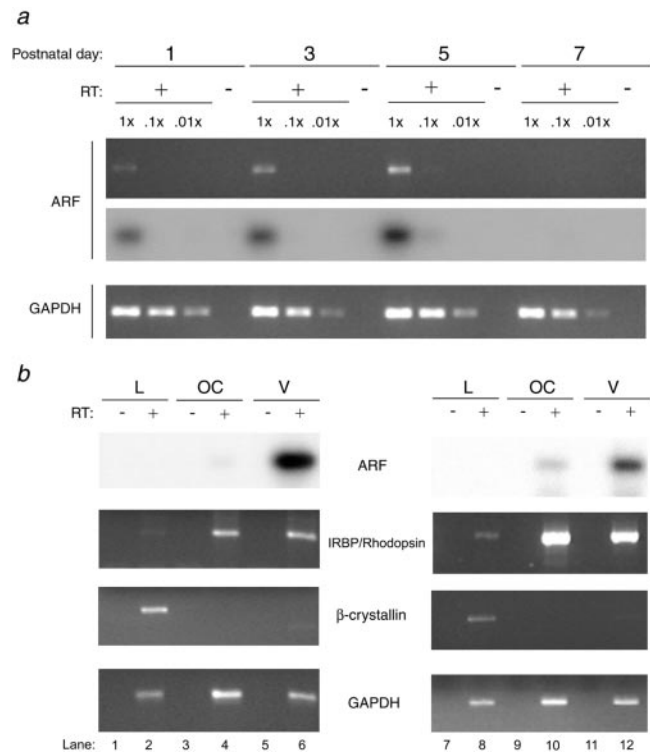
and spatial pattern of Arf expression in the postnatal eye. Increasing expression of Arf was detectable by RT-PCR, using RNA from whole eyes at P1 through P5, whereas at P7 and P9 Arf expression was undetectable (Fig. 3*a* and data not shown). To determine which part of the eye contained Arf-expressing cells, we used RT-PCR to amplify RNA from gross fractions that contained the lens, the optic cup, or the remaining amorphous vitreous. With this assay, we routinely isolated fractions of the eye that expressed lens-specific genes such as β-crystallin; Arf was not expressed in these fractions (Fig. 3*b*, lanes 1, 2, 7, and 8). Gross fractions of the eye that were derived from the vitreous always were contaminated with tissue that expressed neuro-retina-specific genes, such as rhodopsin and interphotoreceptor retinoid-binding protein (Fig. 3*b*, lanes 5, 6, 11, and 12). Despite the contamination of the vitreous with optic cup elements, the fraction that was derived from the vitreous expressed the highest levels of Arf (Fig. 3*b*, lanes 5, 6, 11, and 12 vs. 3, 4, 9, and 10). Together, these findings indicate that Arf is expressed in cells within the vitreous but not in the optic cup or lens at P5. Thus, the timing of Arf induction up to P5 and its localization to the vitreous are consistent with Arf-dependent regulation of VHP regression.

PHPV in $Arf^{-/-}$ Eyes. Failed regression of the HVS underlies a developmental eye disease known as PHPV (24, 25). PHPV is
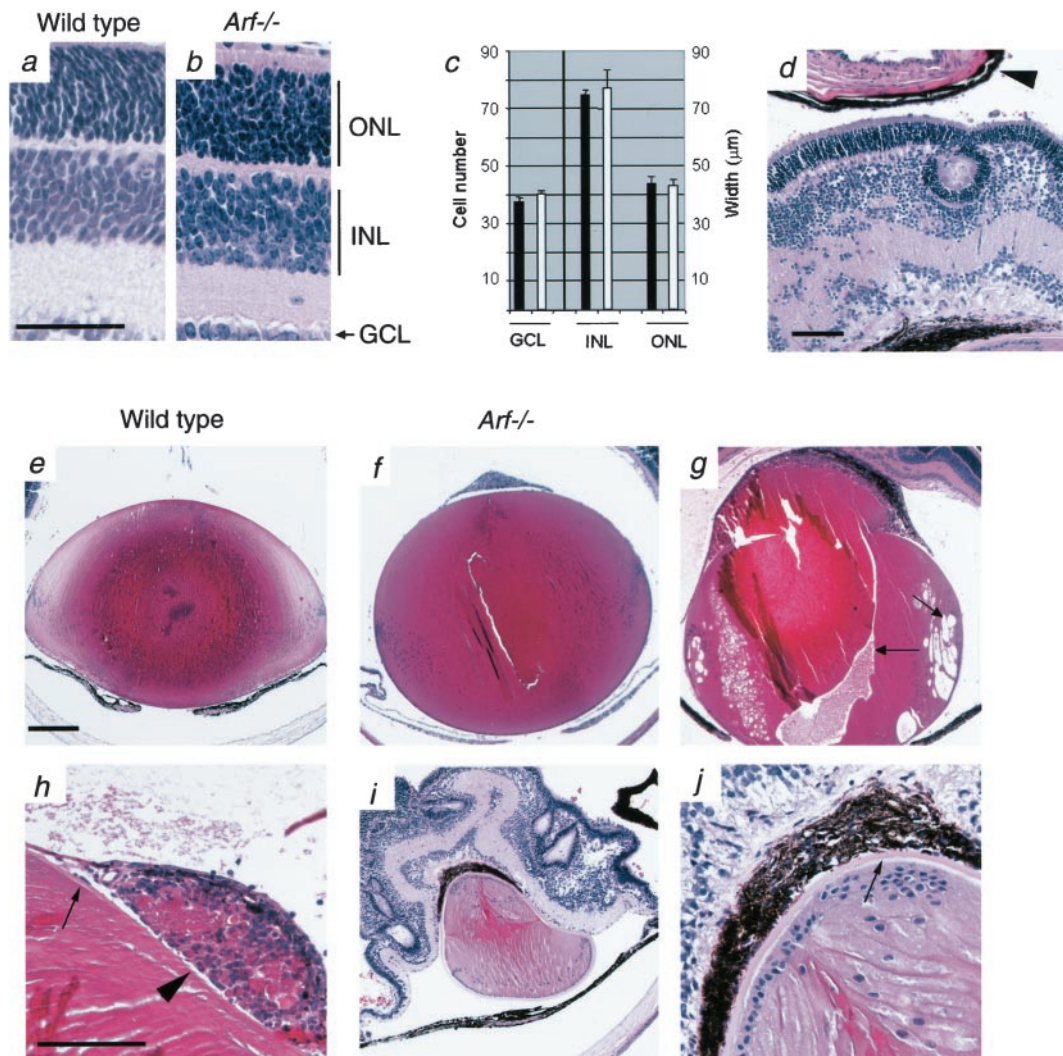
Fig. 4. PHPV-like abnormalities develop in $Arf^{-/-}$ mouse eyes. Photomicrographs (*a*, *b*, and *d–j*) and quantitative measurements (*c*) of eyes from wild-type (*a* and *e*) and $Arf^{-/-}$ (*b*, *d*, and *f–j*) mice at ages P10 (*a*, *b*, *e*, and *f*), P14 (*g* and *h*), and 2 months (*d*, *i*, and *j*). Note the presence of dysplastic changes in the neuroretina (*d* and *i*), detachment of the neuroretina from retina pigment epithelium (arrowhead, *d*), the normal appearance of the $Arf^{-/-}$ lens at P10 (*f* vs. *e*), $Arf^{-/-}$ lens degeneration (arrows, *g*) associated with lens capsule (arrow, *h*) disruption (arrowhead, *h*) at P14, and $Arf^{-/-}$ lens repair (*i* and *j*) associated with posterior lens epithelial cells and regenerated lens capsule (*j*, arrow). ONL, outer nuclear layer; INL, inner nuclear layer; GCL, ganglion cell layer. [Magnifications: ×400 (*a* and *b*), ×100 (*d*), ×40 (*e*, *f*, *g*, and *i*), and ×200 (*h* and *j*); bars = 50 μm (*a*), 100 μm (*d* and *h*), and 250 μm (*e*).] (*c*) Quantitative analysis of the number of ganglion cells within 250 μm of optic nerve and the thickness of INL and ONL within 250 μm of optic nerve in wild-type and $Arf^{+/-}$ (solid bars) or $Arf^{-/-}$ (open bars) mice. Values represent the mean and SEM (error bars).

characterized by microphthalmia and the presence of retrolental fibrovascular tissue that adheres to the inner aspect of the neuroretina and to the posterior aspect of the lens, resulting in retinal abnormalities and cataractous lens degeneration, respectively (24). Because we observed failed HVS regression in $Arf^{-/-}$ mouse eyes, we determined whether there were other pathological changes that resembled PHPV.

Between P1 and P10, with the exception of occasionally observing single retinal folds, the neuroretina of $Arf^{-/-}$ mice was morphologically similar to that of wild-type mice (Figs. 1 *a–d* and 4 *a* and *b*) or $Arf^{+/-}$ (data not shown) littermates. At P10, the size and cellularity of the developing outer and inner nuclear and ganglion cell layers were similar in wild-type and $Arf^{-/-}$ mice (Fig. 4 *a–c*). However, at P14 and beyond, the $Arf^{-/-}$ neuroretina was markedly abnormal, as evidenced by the presence of retinal folds (Fig. 1*f*), rosette-like arrangements of dysplastic photoreceptor cells (Fig. 4 *d* and *i*), progressive physical attachment of the retrolental mass to the neuroretina, in which areas the inner

nuclear and ganglion cell layers were disorganized (Figs. 1*f* and 4 *d* and *i*), and progressive detachment of the neuroretina from the retina pigment epithelium (Fig. 4 *d* and *i*).

The microscopic appearance of the $Arf^{-/-}$ lens also appeared normal up to P10 (Fig. 4 *e* vs. *f*). In addition, the expression of α- and β-crystallin mRNA in the lens was similar in wild-type, $Arf^{+/-}$, and $Arf^{-/-}$ mice at P5 (data not shown). However, at approximately P14, the lens underwent degenerative changes characterized by vacuolization and lens material degradation (Fig. 4*g*). This was associated with attachment of the retrolental tissue to the posterior lens, lens capsule destruction, and extrusion of lens material into the retrolental tissue (Fig. 4 *g* and *h*). Attempted lens repair beyond P14 was manifested by the accumulation of lens epithelial cells lining a regenerated posterior capsule (Fig. 4 *i* and *j*).

The timing of the onset and the progressive nature of the neuroretina and lens abnormalities suggested that they were secondary to the progressive attachment of the retrolental tissue
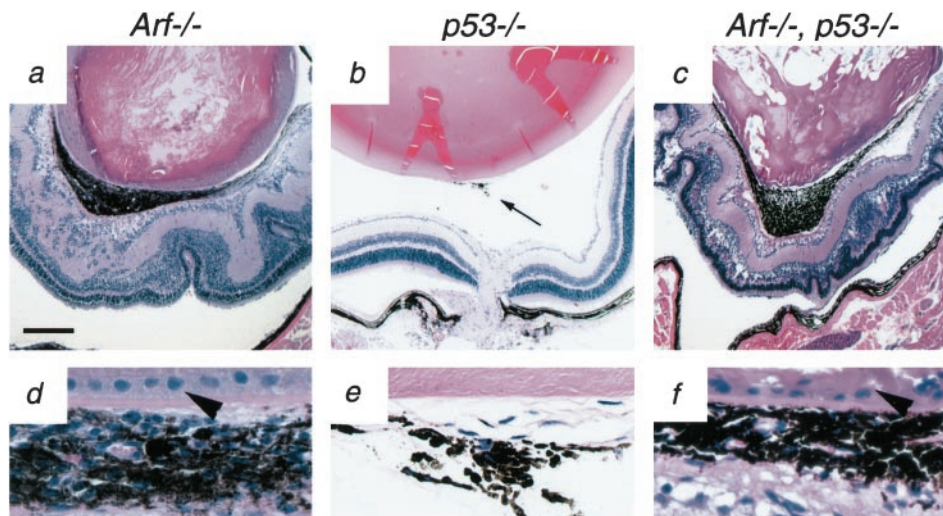
Fig. 5. PHPV in $Arf^{-/-}$ mice is $p53$-independent. Representative photomicrographs (*a–f*) of H&E-stained sections of eyes from 2-month-old $Arf^{-/-}$ (*a* and *d*), $p53^{-/-}$ (*b* and *e*), and $Arf^{-/-}$, $p53^{-/-}$ (*c* and *f*) mice. (*d–f*) Higher magnification of retrolental tissue from corresponding section in *a–c*. Note the presence of pigmented retrolental tissue (*a* and *c*) and posterior lens capsule destruction and repair (arrowheads in *d* and *f*) in $Arf^{-/-}$ and $Arf^{-/-}$, $p53^{-/-}$ eyes whereas minimal retrolental tissue is present (arrow, *b*) and the posterior lens is intact (*e*) in $p53^{-/-}$ eye. Neither retrolental tissue nor lens capsule disruption was observed in age-matched, wild-type mice. [Magnifications: ×40 (*a–c*) and ×400 (*d–f*); bar = 250 μm (*a*).]

to these structures. This constellation of progressive pathologic findings recapitulates those in patients with PHPV (24, 25).

PHPV Develops in $Arf^{-/-}$ Mice Independent of p53. All of the PHPV-like pathologic findings were detected in all $Arf^{-/-}$ eyes ($n = 32$ eyes from 22 mice), but none were observed in $Arf^{+/-}$ littermates ($n = 11$ eyes from eight mice) or wild-type mice ($n = 15$ eyes from 12 mice). The complete penetrance of this phenotype in $Arf^{-/-}$ mice and its complete absence in $Arf^{+/-}$ mice indicated that retention of at least one Arf allele was necessary and sufficient to drive normal HVS regression and prevent PHPV.

Because p19^{Arf} is thought to function largely by stabilizing p53 (7), we considered whether a similar eye phenotype would develop in $p53^{-/-}$ mice in a similar genetic background. To address this, we examined eyes from 2- to 4-month-old $p53^{-/-}$ mice ($n = 14$ eyes from nine mice). The eyes of $p53^{-/-}$ mice were often normal. However, we occasionally observed several layers of retrolental cells in $p53^{-/-}$ eyes (Fig. 5*b*), a finding that is consistent with slowed or incomplete HVS regression in some mice (34, 35). Importantly, we have not observed lens capsule disruption (Fig. 5 *e* vs. *d*) or other PHPV-like abnormalities in $p53^{-/-}$ mice. To demonstrate further that the $Arf^{-/-}$ eye abnormalities did not depend on p53, we evaluated the eyes of $Arf^{-/-}$, $p53^{-/-}$ mice ($n = 5$ eyes from three mice). The loss of $p53$ did not alter the $Arf^{-/-}$ eye phenotype (Fig. 5 *a–f*). Therefore, Arf regulates HVS regression and prevents PHPV in a manner that is independent of $p53$.

Discussion

These studies demonstrate that Arf is required for the normal regression of the HVS during the postnatal maturation of the primary vitreous of the eye. The persistent HVS and surrounding perivascular retrolental tissue caused secondary pathologic processes that disrupted the neuroretina and the lens. The phenotype was completely penetrant in $Arf^{-/-}$ mice and strictly independent of $p53$. These findings provide compelling evidence for a $p53$-independent function of Arf as a mediator of vascular regression during mouse eye development.

The $Arf^{-/-}$ eye abnormalities closely resembled those in PHPV, which often is suspected because of microphthalmia and

is associated with failed HVS regression (25). Eyes from patients with PHPV have the following pathologic characteristics: (*i*) the presence of retrolental tissue, which can contain melanocytes; (*ii*) the attachment of the retrolental tissue to the inner neuroretina; (*iii*) retrolental tissue-induced traction on the neuroretina that causes neuroretina detachment from the retina pigment epithelium; (*iv*) cellular disorganization and other dysplastic changes in the neuroretina; (*v*) posterior lens capsule destruction by the retrolental mass; and (*vi*) cataractous degeneration of the lens (24, 25, 36, 37). The observation that the eye pathology in $Arf^{-/-}$ mice is similar to that in PHPV patients raises the question of whether ARF abnormalities may contribute to this disease. Reports of familial cases (38–40) and bilateral eye disease (24) suggest that there may be a genetic basis for PHPV. If PHPV were caused by ARF abnormalities, because it is usually unilateral and sporadic (24, 25), ARF disruption likely would occur as a somatic cell event before or during eye development.

Our results offer insight into the cellular and genetic mechanisms that control HVS regression and prevent the development of PHPV. HVS regression involves apoptosis in endothelial cells (31, 34) and pericytes (41). This apoptosis is at least partially $p53$-dependent because HVS regression is slowed or incomplete in inbred $p53^{-/-}$ BALB/c (34) and C57BL/6 (35) mice. Yet, incomplete HVS regression is not sufficient to cause the full manifestations of PHPV, which occur only variably in these inbred $p53^{-/-}$ mice and did not occur in our mixed C57BL/6 × 129/Sv $p53^{-/-}$ mice with residual HVS. In contrast, PHPV was completely penetrant in our mixed C57BL/6 × 129/Sv $Arf^{-/-}$ mice, which suggested that the mechanisms allowing PHPV to develop may be regulated by p19^{Arf}.

Apoptosis in the HVS peaks between P7 and P8 in the mouse (34) and the VHP regresses between P6 and P10 (31). Because Arf was expressed in the vitreous from P1 through P5 (our data), it seems unlikely that it directly promotes apoptosis during VHP regression. The principal $Arf^{-/-}$ eye abnormality was the presence of perivascular fibroblastic cells within the VHP. By virtue of their perivascular location and fibroblastic morphology, they may represent pericyte-like cells that were excessively proliferating, as evidenced by Ki-67 staining. Arf expression arrests the proliferation of cultured fibroblasts (27), and cultured $Arf^{-/-}$ mouse embryo fibroblasts proliferate continuously (26). Al-

though it is possible that the presence of the perivascular cells is caused by *Arf*-dependent abnormalities in cellular differentiation, migration, or apoptosis, the simplest interpretation is that *Arf* normally functions from P1 through P5 to prevent their proliferation.

Pericytes stabilize developing vessels by expressing *Ang-1* and *VEGF* (4, 6, 42–44). Small vessels of the VHP normally are covered incompletely by pericytes (30, 31). In principle, this would destabilize the underlying vasculature and may allow for its regression. We have not observed *Arf*-dependent changes in the level of either *Ang-1* or *VEGF* mRNA from P1 through P9 in wild-type mouse eyes or in *Arf*$^{-/-}$ mouse eyes (data not shown). We cannot exclude the possibility, however, that *Arf* expression in perivascular cells may regulate Ang-1 or VEGF protein or the expression of other angiogenic genes to promote VHP regression and prevent PHPV.

Perhaps the most intriguing potential implication of our findings relates to the tumor suppressor activity of p19^{Arf}. We have shown that *Arf* is required to promote vascular regression in the developing eye. Factors that shift the balance of pro- and antiangiogenic factors in favor of angiogenesis or away from vascular regression can contribute to malignant tumorigenesis (2, 3, 45). Although the molecular mechanisms are not presently clear, we speculate that the loss of *Arf* in tumor cells or in host perivascular cells might indirectly facilitate tumor development by favoring the "angiogenic switch" (3).

1. Folkman, J. (1995) *Nat. Med.* **1,** 27–31.
2. Hanahan, D. & Weinberg, R. A. (2000) *Cell* **100,** 57–70.
3. Hanahan, D. & Folkman, J. (1996) *Cell* **86,** 353–364.
4. Risau, W. (1997) *Nature (London)* **386,** 671–674.
5. Saaristo, A., Karpanen, T. & Alitalo, K. (2000) *Oncogene* **19,** 6122–6129.
6. Yancopoulos, G. D., Davis, S., Gale, N. W., Rudge, J. S., Wiegand, S. J. & Holash, J. (2000) *Nature (London)* **407,** 242–248.
7. Sherr, C. J. (1998) *Genes Dev.* **12,** 2984–2991.
8. Levine, A. J. (1997) *Cell* **88,** 323–331.
9. Dameron, K. M., Volpert, O. V., Tainsky, M. A. & Bouck, N. (1994) *Science* **265,** 1582–1584.
10. Mukhopadhyay, D., Tsiokas, L. & Sukhatme, V. P. (1995) *Cancer Res.* **55,** 6161–6165.
11. Zhang, L., Yu, D., Hu, M., Xiong, S., Lang, A., Ellis, L. M. & Pollock, R. E. (2000) *Cancer Res.* **60,** 3655–3661.
12. Giaccia, A. J. & Kastan, M. B. (1998) *Genes Dev.* **12,** 2973–2983.
13. Momand, J., Zambetti, G. P., Olson, D. C., George, D. L. & Levine, A. J. (1992) *Cell* **69,** 1237–1245.
14. Oliner, J. D., Pietenpol, J. A., Thiagalingam, S., Gyuris, J., Kinzler, K. W. & Vogelstein, B. (1993) *Nature (London)* **362,** 857–860.
15. Haupt, Y., Maya, R., Kazaz, A. & Oren, M. (1997) *Nature (London)* **387,** 296–299.
16. Kubbutat, M. H. G., Jones, S. N. & Vousden, K. H. (1997) *Nature (London)* **387,** 299–303.
17. Kamijo, T., Weber, J. D., Zambetti, G., Zindy, F., Roussel, M. F. & Sherr, C. J. (1998) *Proc. Natl. Acad. Sci. USA* **95,** 8292–8297.
18. Pomerantz, J., Schreiber-Agus, N., Liegeois, N. J., Silverman, A., Alland, L., Chin, L., Potes, J., Chen, K., Orlow, I., Lee, H.-W., *et al.* (1998) *Cell* **92,** 713–723.
19. Zhang, Y., Xiong, Y. & Yarbrough, W. G. (1998) *Cell* **92,** 725–734.
20. Kamijo, T., Bodner, S., van de Kamp, E., Randle, D. H. & Sherr, C. J. (1999) *Cancer Res.* **59,** 2217–2222.
21. Donehower, L. A., Harvey, M., Slagle, B. L., McArthur, M. J., Montgomery, C. A., Jr., Butel, J. S. & Bradley, A. (1992) *Nature (London)* **356,** 215–221.
22. Jacks, T., Remington, L., Williams, B. O., Schmitt, E. M., Halachmi, S., Bronson, R. T. & Weinberg, R. A. (1994) *Curr. Biol.* **4,** 1–7.
23. Weber, J. D., Jeffers, J. R., Rehg, J. E., Randle, D. H., Lozano, G., Roussel, M. F., Sherr, C. J. & Zambetti, G. P. (2000) *Genes Dev.* **14,** 2358–2365.
24. Haddad, R., Font, R. L. & Reeser, F. (1978) *Surv. Ophthalmol.* **23,** 123–134.
25. Goldberg, M. F. (1997) *Am. J. Ophthalmol.* **124,** 587–626.
26. Kamijo, T., Zindy, F., Roussel, M. F., Quelle, D. E., Downing, J. R., Ashmun, R. A., Grosveld, G. & Sherr, C. J. (1997) *Cell* **91,** 649–659.
27. Quelle, D. E., Zindy, F., Ashmun, R. A. & Sherr, C. J. (1995) *Cell* **83,** 993–1000.
28. Furukawa, T., Morrow, E. M., Li, T., Davis, F. C. & Cepko, C. L. (1999) *Nat. Genet.* **23,** 466–470.
29. Ring, B. Z., Cordes, S. P., Overbeek, P. A. & Barsh, B. S. (2000) *Development (Cambridge, U.K.)* **127,** 307–317.
30. Zhu, M., Provis, J. M. & Penfold, P. L. (1999) *Exp. Eye Res.* **68,** 553–563.
31. Ito, M. & Yoshioka, M. (1999) *Anat. Embryol.* **200,** 403–411.
32. Hirschi, K. K. & D'Amore, P. A. (1996) *Cardiovasc. Res.* **32,** 687–698.
33. Nehls, V. & Drenckhahn, D. (1991) *J. Cell Biol.* **113,** 147–151.
34. Reichel, M. B., Ali, R. R., D'Esposito, F., Clarke, A. R., Luther, P. J., Bhattacharya, S. S. & Hunt, D. M. (1998) *Cell Death Differ.* **5,** 156–162.
35. Ikeda, S., Hawes, N. L., Chang, B., Avery, C. S., Smith, R. S. & Nishina, P. M. (1999) *Invest. Ophthalmol. Visual Sci.* **40,** 1874–1878.
36. Reese, A. B. (1955) *Am. J. Ophthalmol.* **40,** 317–331.
37. Pollard, Z. F. (1997) *Trends Am. Ophthalmol. Soc.* **95,** 487–549.
38. Lin, A. E., Biglan, A. W. & Garver, K. L. (1990) *Ophthalmol. Pediatr. Genet.* **11,** 121–122.
39. Wang, M. K. & Phillips, C. I. (1973) *Acta Ophthalmol.* **51,** 434–437.
40. Yu, Y. S. & Chang, B. L. (1997) *Korean J. Ophthalmol.* **11,** 123–125.
41. Taniguchi, H., Kitaoka, T., Gong, H. & Amemiya, T. (1999) *Ann. Anat.* **181,** 555–560.
42. Benjamin, L. E., Hemo, I. & Keshet, E. (1998) *Development (Cambridge, U.K.)* **125,** 1591–1598.
43. Reinmuth, N., Liu, W., Jung, Y. D., Ahmad, S. A., Shasheen, R. M., Fan, F., Bucana, C. D., McMahon, G., Gallick, G. E. & Ellis, L. M. (2001) *FASEB J.* **15,** 1239–1241.
44. Folkman, J. & D'Amore, P. A. (1996) *Cell* **87,** 1153–1155.
45. Carmeliet, P. & Jain, R. K. (2000) *Nature (London)* **407,** 249–257.

MEDICAL SCIENCES